by interactions between the RGD site in fibronectin and its integrin-type cell surface receptor. They also imply that these phospholipid surfaces can support a natural cell adhesion process (i.e., specific biochemical recognition).

Chemisorbed phospholipid monolayers, of the type described herein, should provide an attractive framework from which to covalently append adhesion-promoting ligands and to investigate, *quantitatively*, ligand–cell surface interactions, in the presence of nonadhesive proteins (e.g., albumin). Studies that are now in progress are being aimed at synthesizing derivatized CPMs for such use, where particular attention is being focused on the influence of ligand density and peptide sequence on the cell adhesion process.

Registry No. 1, 93404-44-5; 2, 116307-29-0; 3, 122862-88-8; GRGDS, 96426-21-0; Au, 7440-57-5; 16-bromohexadecanoic acid, 2536-35-8; 16-hexadecanolide, 109-29-5; 16-mercaptohexadecanoic acid, 69839-68-5; 2,2′-dipyridyl disulfide, 2127-03-9; 16-(2-pyridyldithio)hexadecanoic acid, 123265-49-6; 1,2-bis[16-(2-pyridydithio)hexadecanoyl)-*sn*-glycerol-3-phosphocholine, 123265-50-9; *sn*-glycero-3-phosphorylcholine, 28319-77-9; 1-palmitoyl-2-[16-(2-pyridyldithio)hexadecanoyl]-*sn*-glycero-3-phosphocholine, 123265-51-0; 1-palmitoyl-*sn*-glycero-3-phosphocholine, 12364-16-8.

Synthesis, Characterization, Theoretical Modeling, and Polymerization of New Fluorophore-Containing Derivatives of Thiophene and Pyrrole

Sanjay Basak, Kasinath Nayak, Dennis S. Marynick,* and Krishnan Rajeshwar*

Center for Advanced Polymer Research, Department of Chemistry, The University of Texas at Arlington, Arlington, Texas 76019

Received June 16, 1989

Two new derivatives of thiophene and pyrrole containing an anthracene model fluorophoric core were synthesized and characterized by NMR and IR spectroscopies, elemental analyses, voltammetry, and spectrofluorometry. Molecular orbital calculations were used to assess the conformational preferences and spin populations of these compounds. The cyclic voltammograms of these compounds contained signatures assignable to both the anthracene and the parent heterocyclic moieties. In this regard, these compounds represent good models for the concept of an electrophoric group discussed in our previous work. In the case of the thiophene derivative, the electrochemistry of the anthracene moiety preceded that of the thiophene ring. Open-shell calculations of the spin density within the unrestricted Hartree–Fock approximation revealed the electron density to be mostly delocalized onto the anthracene moiety. This coupled with unfavorable energetics inhibited polymerization of the thiophene derivative. On the other hand, polymerization of the pyrrole derivative was facile and readily probed by voltammetry. The electroactivity of the polymeric films was investigated with a ferrocene redox probe. In both cases, the fluorescence of the anthracene core was strongly quenched by the polymer backbone.

Introduction

A variety of pyrrole derivatives along with polymers derived from them have been reported in recent years.[1-29] Generally, derivatization begins with substitution at the N center followed by subsequent polymerization utilizing the α and α' positions of the pyrrole ring. An alternative strategy has utilized functionalization (e.g., acylation) of the pendant N–H groups at a polypyrrole surface.[22] A wide range of redox moieties have been incorporated via these two strategies including, for example, ferrocene,[22,25,28,29] $Ru(bpy)_3^{2+}$ (bpy = 2,2′-bipyridyl),[1-3,11,12,20,23] viologens,[5,12,13,17] macrocycles,[10,19,21,24,26,27] phenothiazine,[12,14] copper(II) bipyridyl,[20] $Cu(dpp)_2^+$ (dpp = 2,9-diphenyl-1,10-phenanthroline),[15] anthraquinone,[6] and organic nitroxides.[16] Much less chemistry has been reported for the thiophene system wherein derivatization has been carried out at the β position of the ring to yield either "self-doped" or soluble polymers and oligomers.[30]

In this article, we report the synthesis, characterization, and polymerization of new derivatives of thiophene and pyrrole (1 and 2) containing anthracene as a model fluorophoric core. Molecular orbital calculations were performed to assess the spin densities in the monomeric and

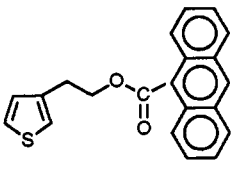

1

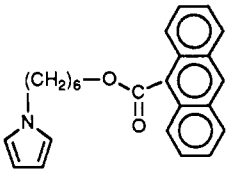

2

dimeric radical cation forms of 1 and 2. These, along with projections of the conformational preferences, aided in the

* Authors to whom correspondence should be directed.

(1) Bidan, G.; Deronzier, A.; Moutet, J. C. *J. Chem. Soc., Chem. Commun.* **1984**, 1185.
(2) Bidan, G.; Deronzier, A.; Moutet, J. C. *Nouv. J. Chim.* **1984**, *8*, 501.
(3) Cosnier, S.; Deronzier, A.; Moutet, J. C. *J. Phys. Chem.* **1985**, *89*, 4895.
(4) Bidan, G., *Tetrahedron Lett.* **1985**, *26*, 735.
(5) Coche, L.; Deronzier, A.; Moutet, J. C. *J. Electroanal. Chem.* **1986**, *198*, 187.
(6) Audebert, P.; Bidan, G.; Lapkowski, G. *J. Chem. Soc., Chem. Commun.* **1986**, 887.
(7) Coche, L.; Moutet, J. C. *J. Electroanal. Chem.* **1987**, *224*, 111.
(8) Coche, L.; Moutet, J. C. *J. Am. Chem. Soc.* **1987**, *109*, 6887.
(9) Deronzier, A.; Essakalli, M.; Moutet, J. C. *J. Chem. Soc., Chem. Commun.* **1987**, 773.
(10) Deronzier, A.; Latour, J.-M. *J. Electroanal. Chem.* **1987**, *224*, 295.
(11) Cosnier, S.; Deronzier, A.; Moutet, J. C. *Inorg. Chem.* **1988**, *27*, 2390.
(12) Downard, A. J.; Surridge, N. A.; Meyer, T. J.; Cosnier, S.; Deronzier, A.; Moutet, J. C. *J. Electroanal. Chem.* **1988**, *246*, 321.

0897-4756/89/2801-0611$01.50/0

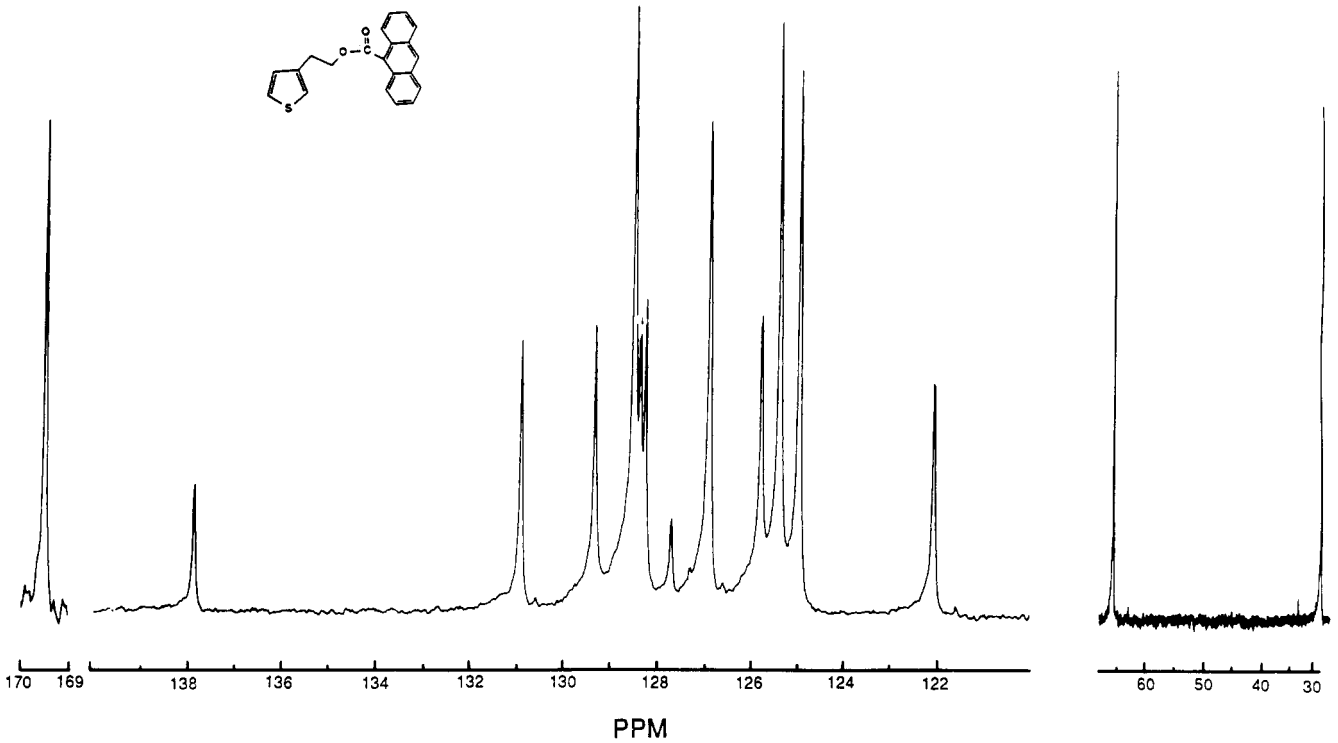

Figure 1. ^{13}C NMR spectrum of 1 in $CDCl_3$.

prediction of the relative susceptibility of 1 and 2 to polymerization. A major impetus for this study was our recent finding[31] that the luminescent emission from probes such as pyrene and $Ru(bpy)_3^{2+}$ could be reversibly modulated by electrochemical control of the oxidation state of a neighboring polypyrrole membrane.

Experimental Section

Synthesis of 1. Anthracene-9-carboxylic acid was mixed with an excess of thionyl chloride, and the slurry was stirred at room temperature for 20 h until a clear yellow solution was obtained. Thionyl chloride was evaporated under reduced pressure to obtain the acid chloride, 3, as a greenish yellow solid.

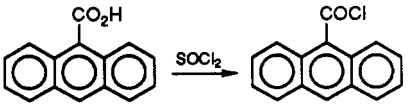

3

2-(3-Thienyl)ethanol (0.54 g, 4.15 mmol) was mixed with 10 mL of anhydrous ether. The system was flushed with nitrogen. *n*-Butyllithium (2 M in hexane) (2.1 mL) was added dropwise to the solution which turned into a white suspension. After 10 min, a solution of 4.15 mmol (1.0 g) of 3 in anhydrous ether was added

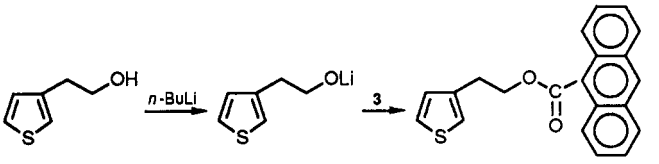

1

to the suspension dropwise through a syringe, and the mixture was stirred for 2 h. The solution was then filtered from inorganic solid. The ether solution was evaporated to obtain a light brown solid. It was recrystallized from ether/petroleum ether to obtain a light yellow solid. Yield: 77%. Mp: 76–77 °C. FTIR (DRIFT) cm^{-1}: 1716 (C=O), 1635, 1624 (aromatic C=C), 1446, 1411 (ring stretch), 1045 (C—O). ^1H NMR ($CDCl_3$) δ: 8.49 (s), 7.89 (m), 7.45 (m), 7.27 (m), 7.08 (m), 4.85 (t), 3.24 (t). ^{13}C NMR ($CDCl_3$) δ: 169.52, 137.85, 130.92, 129.35, 128.52, 128.39, 128.28, 127.72, 126.92, 125.80, 125.41, 124.99, 122.09, 65.52, 29.72. Anal. Calcd for $C_{21}H_{16}O_2S$: C, 75.88; H, 6.85. Found: C, 75.47; H, 4.80.

Figure 1 contains a ^{13}C NMR spectrum of 1 in $CDCl_3$. To deconvolute the complex set of 12 ring C peaks appearing between 138 and 122 ppm (out of the 12, 4 are due to thiophene carbons and 8 are attributable to the anthracene carbons), a separate DEPT (distortionless enhancement by polarization transfer) decoupling experiment was done. This experiment enables assignment of the four peaks (δ: 137.85, 130.92, 128.39, 127.72) to the ring carbons with no attached hydrogen and the other eight carbons to attachment with single hydrogen atoms.

Synthesis of 4.[4] A solution of pyrrole (8.5 g) in 20 mL of THF was slowly added to 50 mL of THF and 4.8 g of potassium in a three-necked flask. The solution was refluxed under N_2 until all

(13) Coche, L.; Moutet, J. C. *J. Electroanal. Chem.* **1988**, *245*, 313.
(14) Deronzier, A.; Essakalli, M.; Moutet, J. C. *J. Electroanal. Chem.* **1988**, *244*, 163.
(15) Bidan, G.; Divisia-Blohorn, B.; Kern, J. M.; Sauvage, J. P. *J. Chem. Soc., Chem. Commun.* **1988**, 723.
(16) Audebert, P.; Bidan, G.; Lapkowski, M.; Limosin, D. in *Electronic Properties of Conjugated Polymers*; Kuzmany, H., Mehring, M., Roth, S., Eds; Springer-Verlag Series; Springer-Verlag: New York, 1987, Vol. 76, pp 366–384. See also references therein.
(17) Shu, C. F.; Wrighton, M. S. *J. Phys. Chem.* **1988**, *92*, 5221.
(18) Haimerl, A.; Merz, A. *Angew. Chem., Intl. Ed. Engl.* **1986**, *25*, 180.
(19) Okabayashi, K.; Ikeda, O.; Tamura, H. *J. Chem. Soc., Chem. Commun.* **1983**, 684.
(20) Daire, F.; Bedioui, F.; Devynick, J.; Bied-Charreton, C. *J. Electroanal. Chem.* **1986**, *205*, 309.
(21) Bedioui, F.; Bongars, C.; Devynick, J.; Bied-Charreton, C.; Hinnen, C. *J. Electroanal. Chem.* **1986**, *207*, 87.
(22) Rosenthal, M. V.; Skotheim, T.; Warren, J. *J. Chem. Soc., Chem. Commun.* **1985**, 342.
(23) Eaves, J. G.; Munro, H. S.; Parker, D. *J. Chem. Soc., Chem. Commun.* **1985**, 684.
(24) Skotheim, T.; Rosenthal, M. V.; Linkous, C. A. *J. Chem. Soc., Chem. Commun.* **1985**, 612.
(25) Eaves, J. G.; Munro, H. S.; Parker, D. *Synth. Met.* **1986**, *16*, 123.
(26) Rosenthal, M. V.; Skotheim, T. A.; Linkous, C. A. *Synth. Met.* **1986**, *15*, 219.
(27) Collin, J. P.; Sauvage, J. P. *J. Chem. Soc., Chem. Commun.* **1987**, 1075.
(28) Inagaki, T.; Hunter, M.; Yang, X. Q.; Skotheim, T. A.; Okamoto, Y. *J. Chem. Soc., Chem. Commun.* **1988**, 126.
(29) Foulds, N. C.; Lowe, C. R. *Anal. Chem.* **1988**, *60*, 2473.
(30) For a review, see: Bidan, G.; Ehui, B.; Lapkowski, M. *J. Phys. D* **1988**, *21*, 1043. Also see: Patel, A. O.; Ikenoue, Y.; Wudl, F.; Heeger, A. J. *J. Am. Chem. Soc.* **1987**, *109*, 1858. Reynolds, J. R.; Sundaresan, N. S.; Pomerantz, M.; Basak, S.; Baker, C. K. *J. Electroanal. Chem.* **1988**, *250*, 355.
(31) Tsai, E. W.; Phan, L.; Rajeshwar, K. *J. Chem. Soc., Chem. Commun.* **1988**, 771.

the potassium was reacted. The resulting mixture was cooled to

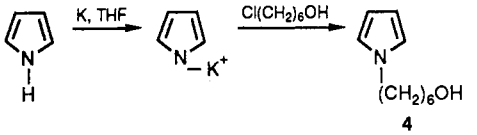

4

room temperature, and a solution of 6-chloro-1-hexanol (8.2 g) in 20 mL of THF was slowly added. After being stirred for 30 min, the solution was poured into 100 mL of ice water and extracted several times with Et_2O. The ether solution was dried over anhydrous Na_2SO_4 and removed by rotary evaporation to obtain the product, **4**. Yield: 6.95 g (70%). ^1H NMR ($CDCl_3$) δ: 6.71 (t, 2 H), 6.20 (t, 2 H), 3.73 (t, 2 H), 3.50 (t, 2 H), 2.10 (s, 1 H), 1.8–1.43 (m, 8 H).

Synthesis of 2. To a solution of **4** (0.69 g) in 20 mL of anhydrous ether, *n*-butyllithium (2 M in hexane) (2.1 mL) was added dropwise at room temperature. After 10 min, a solution of 1.0 g of 9-anthracenecarbonyl chloride, **3**, in 10 mL of ether was added,

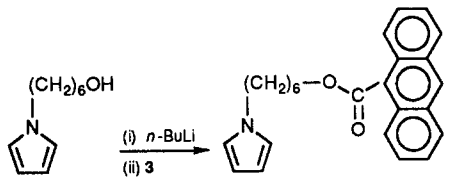

2

and this mixture was stirred for 2 h. The mixture was poured into ice water and extracted with methylene chloride. The extract was dried over anhydrous Na_2SO_4, and the solvent was removed by rotary evaporation to obtain a dark tan solid. It was purified by silica gel column chromatography, and the ester was obtained as a light yellow solid. (the sample was unstable in air.) Yield: 60%. ^1H NMR ($CDCl_3$) δ: 8.50 (s, 1 H), 8.01 (t, 4 H), 7.56–7.45 (m, 4 H), 6.61 (t, 2 H), 6.12 (t, 2 H), 4.61 (t, 2 H), 3.51 (t, 2 H), 1.79 (m, 4 H), 1.51 (m, 4 H). ^{13}C NMR ($CDCl_3$) δ: 169.67, 130.94, 129.20, 128.58, 128.32, 128.04, 126.88, 125.41, 124.91, 120.38, 107.82, 65.61, 44.84, 32.39, 28.59, 26.44, 25.38.

Instrumentation. Electrochemical experiments were performed with an EG&G Princeton Applied Research (PAR) system assembled from Model 173 and Model 175 modules and a Houston Instrument *X–Y* recorder. All measurements were carried out in dry acetonitrile containing either tetrabutylammonium perchlorate (TBAP) or tetrabutylammonium tetrafluoroborate ($TBABF_4$) (0.1 M each as the supporting electrolyte). The solutions were carefully deoxygenated by bubbling ultrapure N_2 in all the cases. Standard three-electrode cell geometry was utilized with either Pt or indium tin oxide as the working electrode, a Pt wire counter electrode, and Ag/Ag^+ (0.1 M $AgNO_3/CH_3CN$) as reference. In some cases, an aqueous Ag/AgCl reference was employed. All potentials below are quoted with respect to the nonaqueous Ag/Ag^+ reference electrode unless stated otherwise.

NMR and FTIR analyses were performed on Bruker MSL-300 and BioRad Digilab Model FTS-40 spectrometers, respectively. A Perkin-Elmer MPF-44 system was used for spectrofluorometry.

Theoretical Calculations. The method of partial retention of diatomic differential overlap (PRDDO)[32-34] was used to partially optimize the geometrics of the systems considered here; this approximate ab initio method has worked well for determining the equilibrium bond lengths in transition-metal compounds.[34,35] We have also previously shown[36,37] how PRDDO is useful for obtaining the geometries of reasonably large molecules similar to the ones considered here. Open-shell calculations were performed within the unrestricted Hartree–Fock (UHF) approximation.[38] All computations were done on the Cray X-MP/24 supercomputer located at the U.T. System Center for High Performance Computing in Austin, TX.

Results and Discussion

Voltammetry of 1 and 2. Figure 2a contains a cyclic voltammogram of **1** at a Pt button electrode in MeCN/0.1 M $TBABF_4$. If the positive potential limit of the voltammetric scan is kept $\lesssim$ +1.40 V, quasi-reversible redox waves at +1.10 and −2.05 V are seen (not shown in Figure 2). Comparison with previous work[39] enables assignment of these waves to the oxidation and reduction of the anthracene moiety to its radical cation and anion, respectively. Scanning to more positive potentials (Figure 2a) causes the appearance of a second oxidation wave centered at $\sim$ +1.50 V, and the loss of electrochemical (and possibly chemical) reversibility of the anthracene redox features. Repetitive scanning past +1.50 V causes systematic diminution of current flow, suggestive of electrode passivation. The wave at +1.50 V is attributable to the oxidation of the thiophene moiety, leading in the case of **1** to a rather poorly electroactive polymeric film (see below). Aside from the above major features in the voltammogram, there are weak waves between 0 and −1.50 V attributable to electrochemical products and/or adventitious impurities in the MeCN such as H_2O. These were not investigated in more detail for the purpose of this study.

Figure 2b contains a cyclic voltammogram of **2** at Pt in MeCN/0.1 M TBAP. The cathodic behavior of the anthracene moiety is similar to that discussed in the preceding paragraph for **1**; the corresponding redox wave also occurs at −2.05 V for **2**. The anodic branch, on the other hand, manifests waves at +0.92, +1.20, and $\sim$ +1.90 V, respectively. Previous work suggests the first wave as being due to the anodic oxidation of the *N*-alkylpyrrole moiety in **2**.[40] The oxidation of the anthracene moiety is shifted somewhat from the **1** case and now occurs at +1.20 V. The wave at $\sim$ +1.90 V is assigned to the "overoxidation" of the pyrrole moiety as reported by previous authors.[41] Arrest of the forward (positive-going) scan just prior to the anthracene wave at +1.20 V identifies the cathodic features with a main wave centered at $\sim$ 0.45 V as being due to the products of the electrolysis of the pyrrole moiety. Specifically, the protons released by the coupling of the pyrrole rings are implicated. As in the case of **1**, minor anodic features on the return scan of the cathodic branch occur between 0 and −1.20 V. These were not explored further.

Taken as a unit, the voltammetric data for **1** and **2** corroborate our previous discussion of the concept of an "electrophoric" group; i.e., a portion of a molecule gives rise to an electrochemical signature that is characteristic of that moiety itself rather than of the molecule as a whole.[42] Within this context, the anthracene moiety, the thiophene ring (in the case of **1**), and the pyrrole portion of **2** may be viewed as electrophoric groups.

Fluorescence of 1 and 2. Both **1** and **2** display fluorescence emission spectra that originate from the anthracene core. Thus, excitation at 317 nm in acetonitrile yields broad structureless fluorescence emission bands with λ_{max} at 460 nm and 465 nm for **1** and **2**, respectively. These

(32) Marynick, D. S.; Lipscomb, W. N. *Proc. Natl. Acad. Sci. U.S.A.* **1982**, *79*, 1341.
(33) Marynick, D. S.; Axe, F. U.; Kirkpatrick, C. M.; Throckmorton, L. *Chem. Phys. Lett.* **1982**, *99*, 406.
(34) Marynick, D. S.; Reid, R. D. *Chem. Phys. Lett.* **1986**, *17*, 124.
(35) Axe, F. U.; Marynick, D. S. *J. Am. Chem. Soc.* **1988**, *110*, 3728 and related references therein.
(36) Martinez, M.; Reynolds, J. R.; Basak, S.; Black, D.; Marynick, D. S.; Pomerantz, M. *J. Polym. Sci., Part B: Polym. Phys.* **1988**, *26*, 911.
(37) Ruiz, J. P.; Nayak, K.; Marynick, D. S.; Reynolds, J. R. *Macromolecules* **1989**, *22*, 1231.
(38) Pople, J. A.; Beveridge, D. L. *Approximate Molecular Orbital Theory*; McGraw-Hill: New York, 1970.
(39) Bard, A. J.; Faulkner, L. R. *Electrochemical Methods*; Wiley: New York, 1980.
(40) For example: Diaz, A. F.; Castillo, J. I.; Logan, J. A.; Lee, W. Y. *J. Electroanal. Chem.* **1981**, *129*, 115.
(41) Beck, F.; Braun, P.; Oberst, M. *Ber. Bunsenges. Phys. Chem.* **1987**, *91*, 967.
(42) Tsai, E. W.; Witczak, M. K.; Rajeshwar, K.; Pomerantz, M. *J. Electroanal. Chem.* **1987**, *236*, 219.

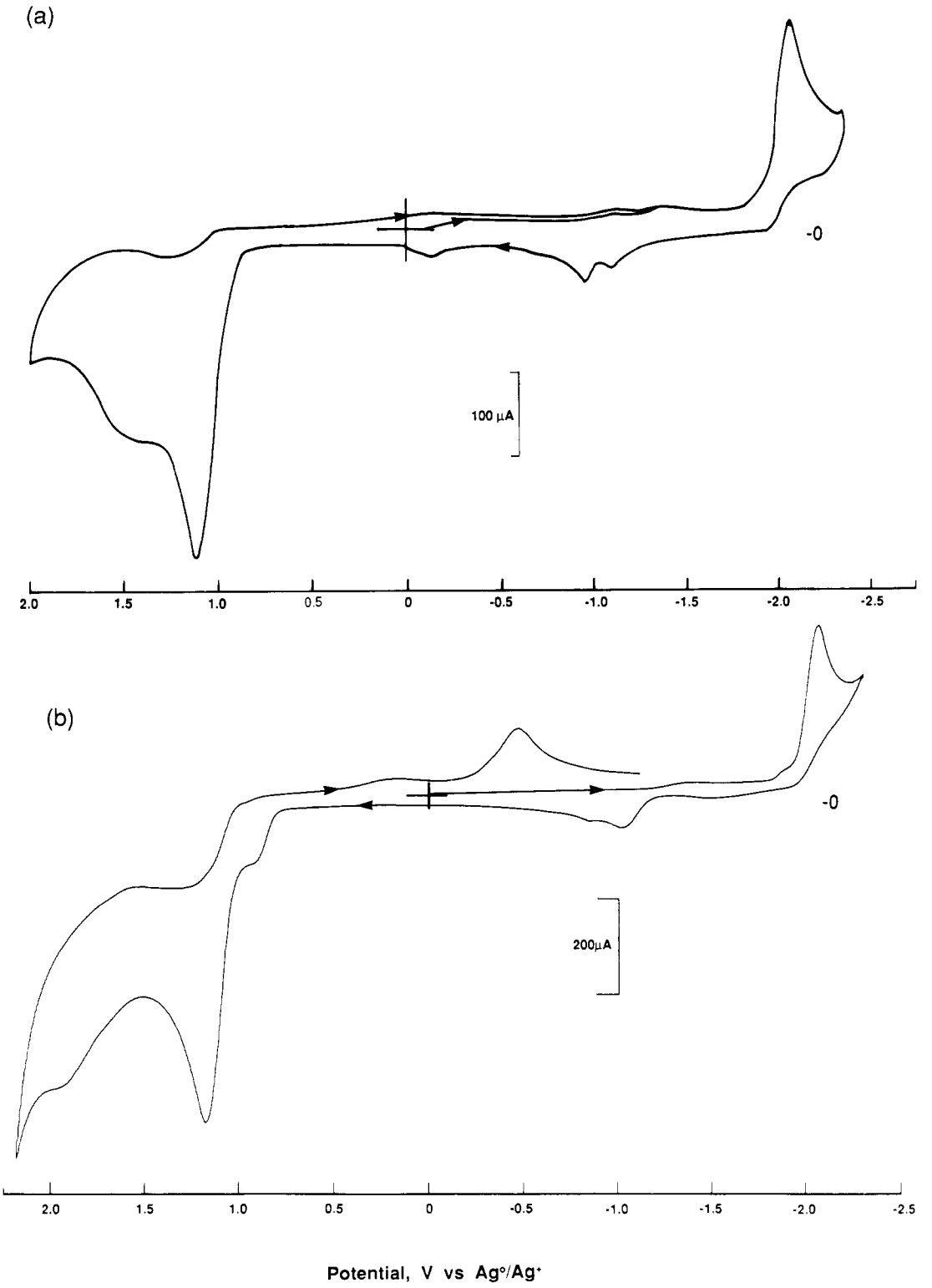

Figure 2. Cyclic voltammograms for 1 (a) and 2 (b) at a Pt button electrode (geometric area: 0.017 cm^2) in MeCN/$TBABF_4$ and MeCN/TBAP, respectively. The potential scan rate was 0.10 V/s.

bands are significantly red-shifted (by ~60 nm) relative to the λ_{max} of anthracene.[43]

Conformation of 1 and 2. For our calculations, we have used the PRDDO-optimized geometries of thiophene and pyrrole monomers[36,37] and the bond lengths and bond angles of anthracene moiety obtained from the experimental findings.[44,45] The bond lengths of the spacer group $(CH_2)_nOC{=}O$ (where n is 2 and 6 for 1 and 2, respectively) are C—O = 1.41 Å, C=O = 1.29 Å, and C—C = 1.53 Å. A planar polymer backbone structure was assumed with C–H bond distances of 1.08 Å. In the case of 1, the bond lengths C5–C4 and C8–C7, the corresponding angle C5–C4–C2, and the rotations about these bonds were optim-

(43) Berlman, I. B. *Handbook of Fluorescence Spectra of Aromatic Molecules*; Academic: New York, 1971; p 356.

(44) Gramaccioli, C. M.; Filippini, G.; Simonetta, M.; Ramdas, S.; Parkinson, G. M.; Thomas, J. M. *J Chem. Soc., Faraday Trans 2* **1980**, *76*, 1336.

(45) Robertson, J. M. *Proc. R. Soc. London, Ser. A* **1933**, *140*, 79.

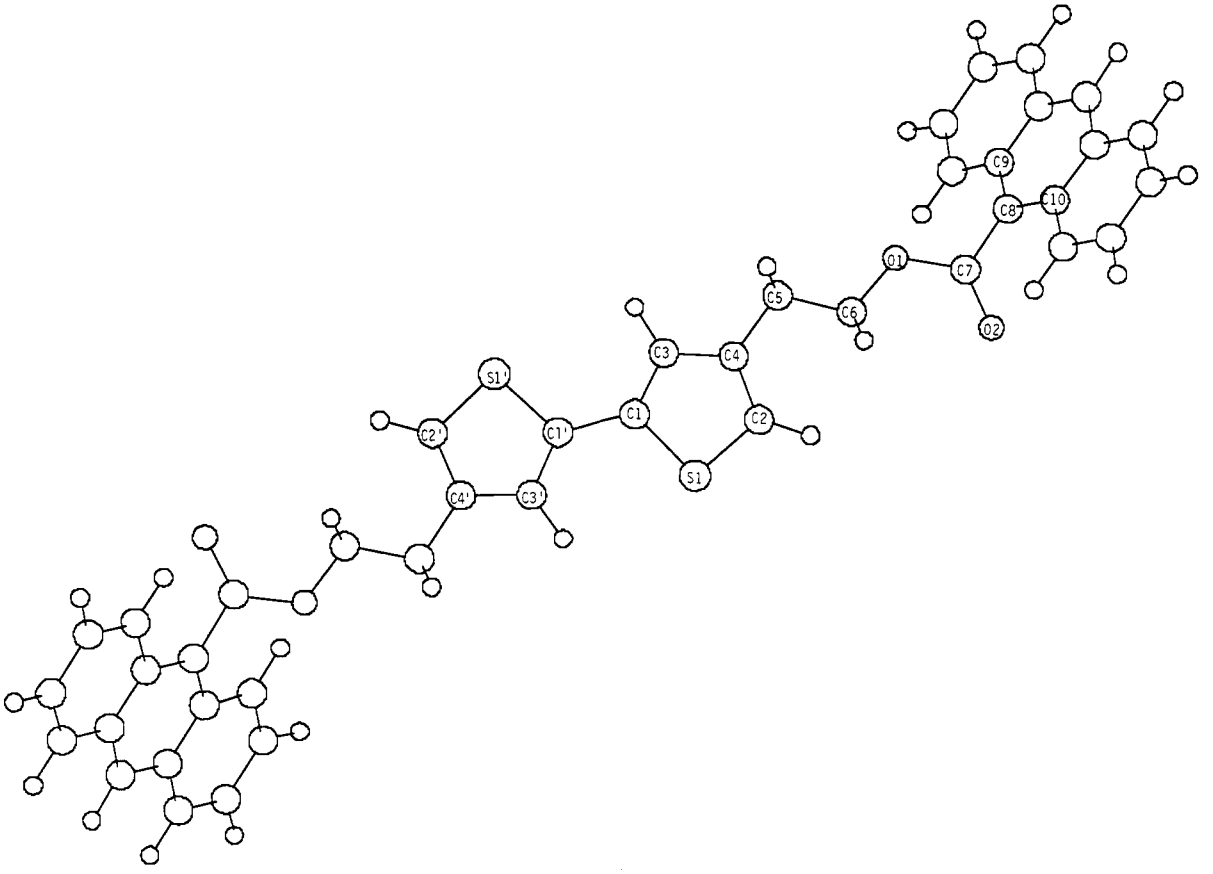

Figure 3. Dimer of 1 constructed from the PRDDO-optimized geometry of the monomer. The spin density distributions on thiophene moiety are C1 = 0.0007e, C2 = −0.0004e, C3 = 0.0005e, and S1 = 0.0009e and the total spin population on the anthracene moiety is ~1.00e.

Table I. PRDDO-Optimized Geometrical Parameters of 1 and 2. The Bond Lengths and Bond Angles Are Given in Angstroms and Degrees, Respectively.

1		2	
C5–C4	1.52	C5–N1	1.48
C8–C7	1.52	C12–C11	1.52
C9–C8–C7	120.0	C13–C12–C11	120.0
C5–C4–C2	123.8	C5–N1–C2	125.5
C1–C1′[a]	1.47	C1–C1′[b]	1.45
C3–C1–C1′[a]	129.9	C3–C1–C1′[b]	122.1
S1–C1–C1′–S1′[a]	180.0	N1–C1–C1′–N1′[b]	180.0

[a,b] Refer to the dimers of 1 and 2, respectively.

ized. Similar optimizations were done for **2**. Specifically, the bond lengths C5–N1 and C12–C11, the bond angle C5–N1–C2, and the rotations about these bonds were taken into consideration for optimization. In both cases, the substituents, $CH_2CH_2OC{=}OAn$ (An = anthracene moiety) in the case of 1 and $(CH_2)_6OC{=}OAn$ in case of **2**, stay planar about the C5–C4 and C5–N1, bonds respectively. The anthracene moiety is twisted with respect to the heterocycle units by about 56° and 58° for 1 and **2**, respectively, with both barriers to internal rotation being 55 kJ/mol. The optimized values of the specified geometrical parameters are given in Table I. The numbering system and the resultant conformation of the dimers are illustrated in Figure 3 and 4 for 1 and **2**, respectively.

Electropolymerization of 1 and 2. Given the importance of dimeric and oligomeric intermediates in the electropolymerization of organic heterocycles (cf. ref 46–48) the majority of calculations focused on dimers of 1 and **2** (cf. Figures 3 and 4). Initial PRDDO UHF calculations on the monomeric radical cation of 1 showed the spin population to be substantially residing on the $CH_2CH_2OC{=}OAn$ substituent. Convergence to a second electronic state with a HOMO predominantly of thiophene character was also achieved; however, the energy of this state was 225 kJ/mol higher than the ground state. These initial calculations highlight the factors that would render polymerization unlikely for 1 in its monomeric radical cation form. Similar conclusions could be reached for the monomeric cation radical of **2**, the energy difference between the electronically perturbed and ground states in this case being ~171 kJ/mol.

Interesting insights into the experimental data to be discussed below are obtained when the dimeric radical cations are theoretically examined for 1 and **2**. The computed spin populations for these species are given in Figures 3 and 4, respectively. In the case of the anodic coupling products from 1, the spin densities at the equivalent α carbons of the thiophene ring are insignificant when compared to the spin population on the anthracene moieties (Figure 3). The energy difference between the state with a HOMO of predominantly anthracene character and the next state with a HOMO of dominant thiophene character was found to be ~99.5 kJ/mol. Thus, a priori, electropolymerization of 1 is expected to be unfavorable *even via the dimeric route*. By way of contrast, the ground state of the dimeric radical cation of **2** shows significant spin densities at the α and α' positions (Figure 4). Note also that the spin population is negligible at the anthracene

(46) Downard, A. J.; Pletcher, D. *J. Electroanal. Chem.* **1986**, *206*, 147.
(47) Hillman, A. R.; Swann, M. J. *Electrochim. Acta* **1988**, *33*, 1303 and references therein.
(48) Baker, C. K.; Reynolds, J. R. *J. Electroanal. Chem.* **1988**, *251*, 307 and references therein.

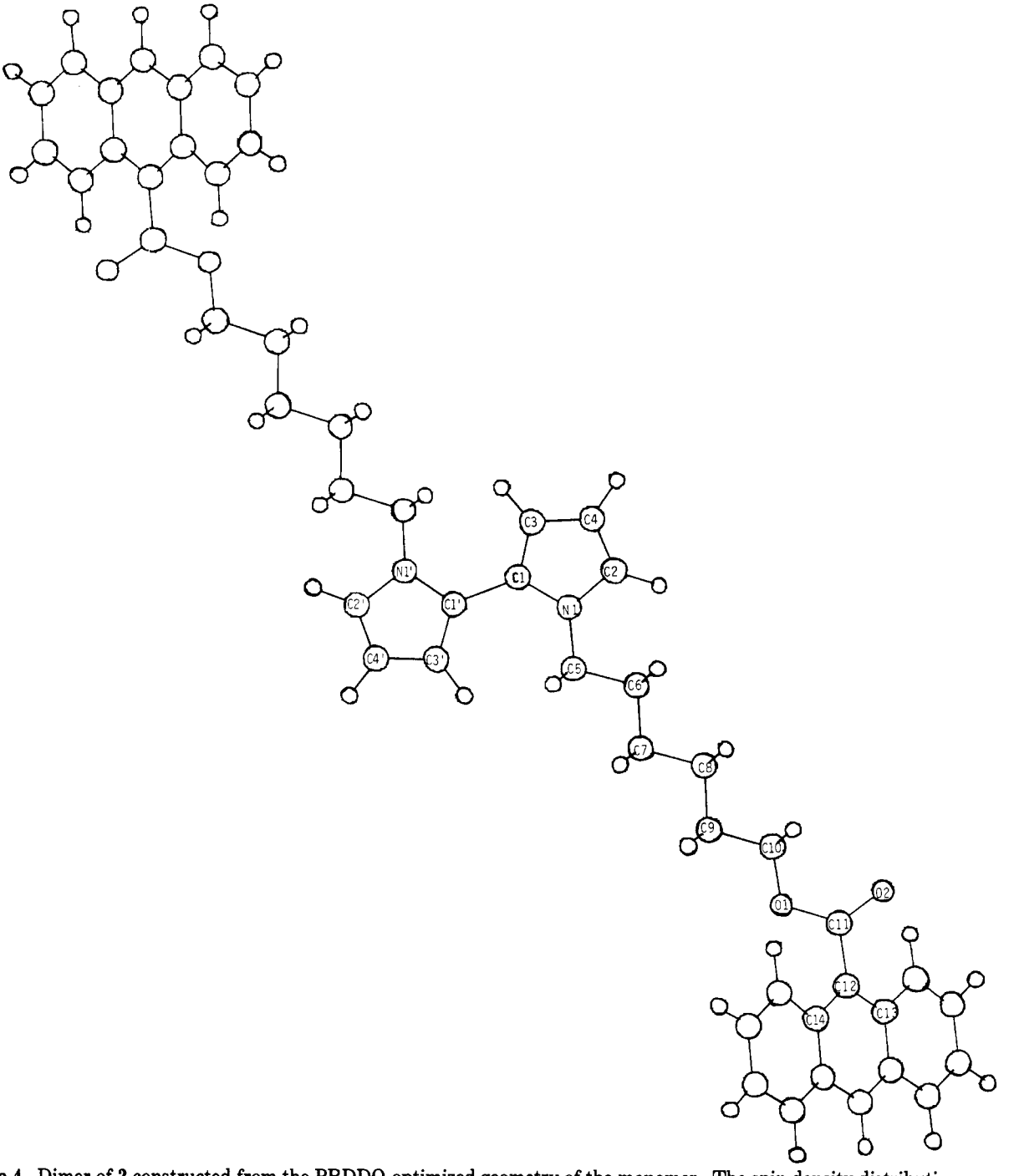

Figure 4. Dimer of **2** constructed from the PRDDO-optimized geometry of the monomer. The spin density distributions on pyrrole moiety are C1 = 0.0001e, C2 = C2′ = 0.678e, C3 = 0.573e, and N1 = −0.209e, and the total spin population on the anthracene moiety is of the order of ~0.01e.

units. Further, the HOMO of pyrrole character is energetically preferred in this case relative to the corresponding state with the anthracene HOMO by ~76 kJ/mol.

Thus, the theoretical calculations lead to the interesting prediction that the electropolymerization via the dimer (or possibly by extension, oligomer) route would be more facile for **2** relative to **1**. This is indeed what we observe in experiments (see below). It must be also pointed out that steric factors are unlikely to be important here, since considerable conformational flexibility exists in the linkage between the anthracene and the heterocycle.

Anodic oxidation of **1** at 2.0 V in MeCN/0.1 M $TBABF_4$ yields a black stream of oligomeric material that diffuses away from the working electrode (either Pt or ITO) surface. Clearly, the products from the electrochemistry of the anthracene moiety preclude efficient thiophene ring coupling and polymer formation. Similar results were obtained with propylene carbonate as the polymerization medium when a potentiostatic film growth mode was employed. Under more forcing conditions, a black electroinactive polymer film is obtained. For example, galvanostatic syntheses at 20–25 mA/cm^2 using 0.1 M **1** in propylene carbonate/0.03 M $TBABF_4$ yields a material that analyzed as follows: S:H:C = 1:14.3:21.02 (theoretical 1:14:21). An FTIR specular reflectance spectrum of this material reveals the expected C=O stretch at ~1732 cm^{-1} amidst a rather high background absorbance.

By way of contrast, the anodic electropolymerization of **2** is much more facile. Figure 5 illustrates the systematic growth of the polymer film on respective cycling of a Pt

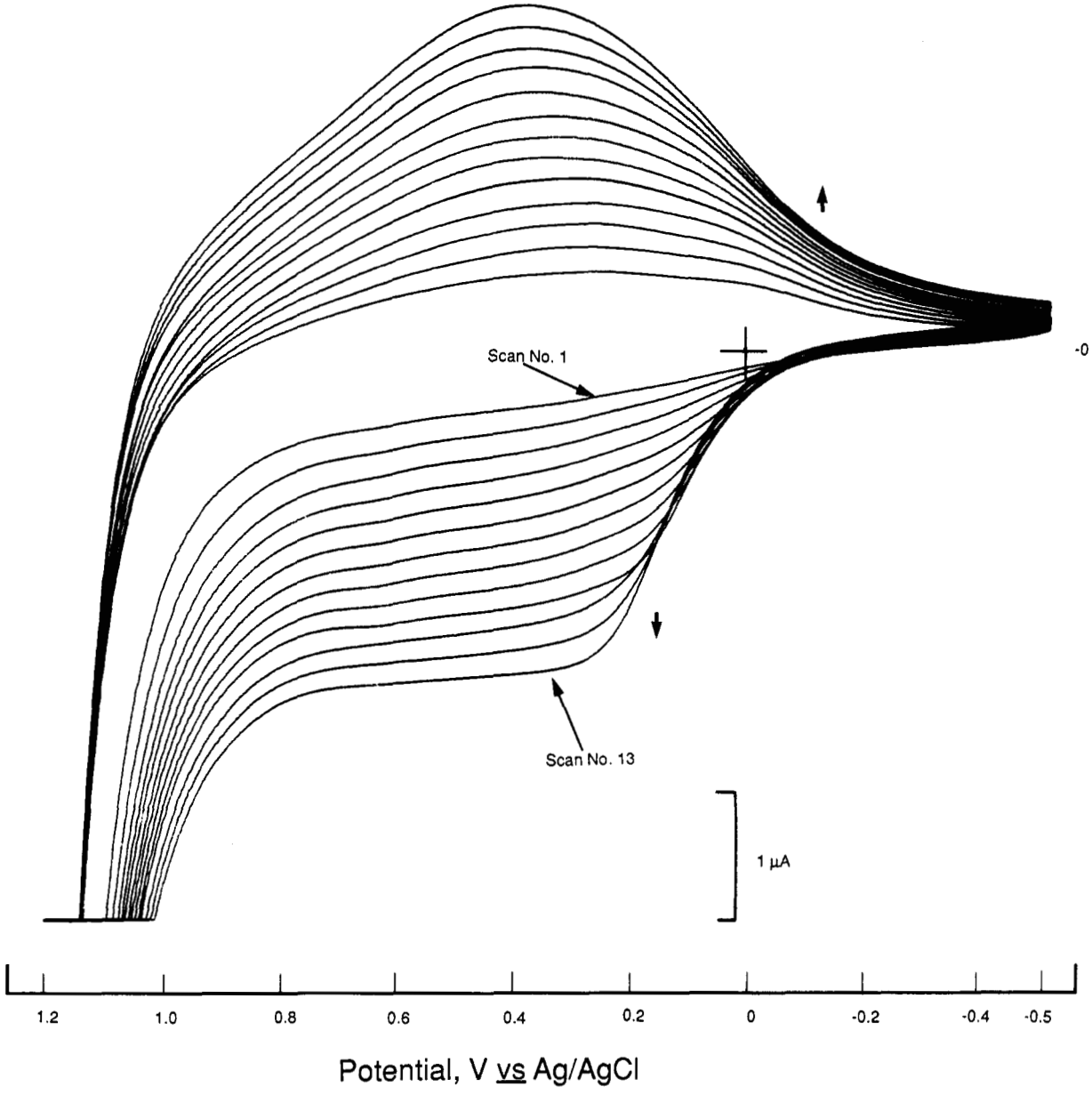

Figure 5. Voltammograms obtained on repetitive cycling of a Pt working electrode between −0.50 and +1.20 V (vs Ag/AgCl) in MeCN/0.1 M TBAP containing 0.1 M **2**. The potential scan rate was 0.10 V/s.

electrode between −0.50 and +1.20 V vs Ag/AgCl in MeCN/0.1 M TBAP containing 0.1 M **2**. For example, under the conditions employed in Figure 5, a polymeric film of **2** may be grown to ~80–100-nm thickness by passage of 33 mC/cm^2 anodic charge.

Transfer of such Pt- or ITO-supported films to a medium containing simply MeCN/TBAP reveals cyclic voltammetric behavior associated with charging and discharging of the polymer film (Figure 6a), when the electrode is cycled between −0.20 and +0.60 V (vs Ag/AgCl). These films are rather unstable on prolonged cycling; for example, the oxidation peak currents are attenuated by ~30% after 50 scans in the electrolyte (Figure 6b). Thus, relative to polypyrrole, the polymer derived from **2** appears to be rather more unstable, although the voltammograms are very similar in shape.

The electroactivity of the polymer film derived from **2** was further explored by using ferrocene as a redox probe.[49] Representative data are contained in Figure 7, which presents cyclic voltammograms at varying scan rates for a Pt electrode cycled between −0.20 and +0.70 V (vs Ag/AgCl) in MeCN/0.1 M TBAP containing 1 mM ferrocene. The anodic oxidation of ferrocene is clearly evident and manifests as a wave at ~0.62 V (vs Ag/AgCl), which is superimposed on the polymer redox background. Interestingly enough, the cathodic waves on the return scan are attenuated, indicating kinetic sluggishness associated with the (mediated) re-reduction of the ferricenium cation. Electron-transfer kinetics limitations also manifest on the forward scan in terms of the systematic positive shift in the anodic wave location at scan rates faster than ~0.02 V/s. The peak currents for the ferrocene oxidation wave are estimated by subtraction of the capacitive contribution from the same electrode in the absence of the electroactive solute in solution. The inset in Figure 7 thus contains a log–log plot of the peak current (for the ferrocene oxidation wave) versus the scan rate. A slope of ~0.6 is obtained, which is intermediate between the values of 1.0 and 0.5 diagnostic of surface-confined[50] and diffusion-limited[39]

(49) Saloma, M.; Aguilar, M. *J. Electrochem. Soc.* **1985**, *132*, 2379.

(50) Laviron, E. *J. Electroanal. Chem.* **1972**, *39*, 1.

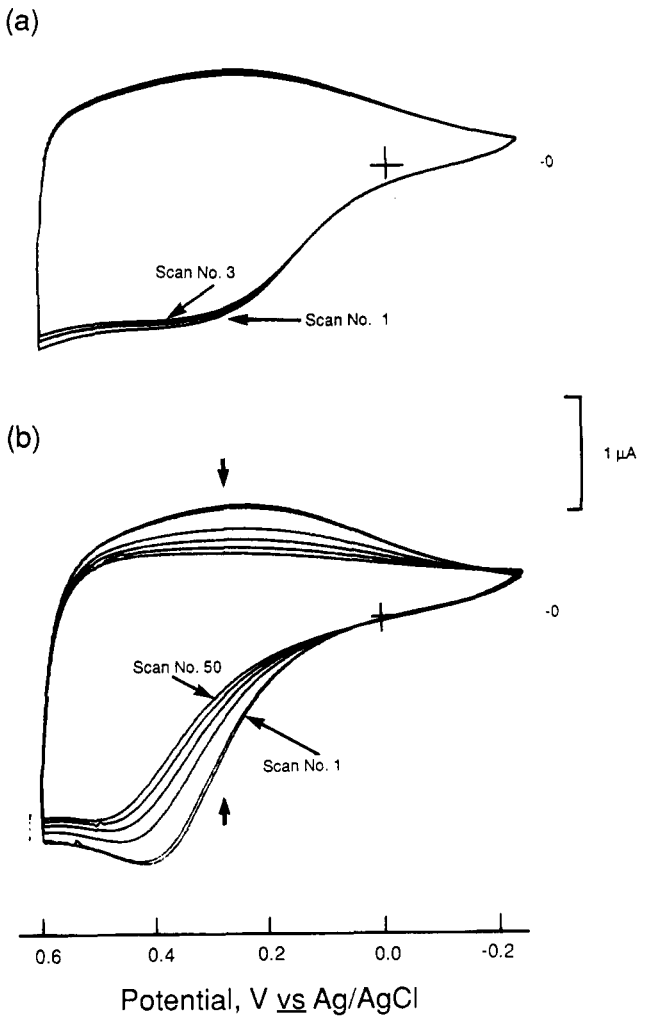

Figure 6. Cyclic voltammogram for poly-2 supported on Pt in MeCN/0.1 M TBAP. The first three scans are shown in a; the influence of prolonged cycling is depicted in b. In both instances, the potential scan rate was 0.05 V/s. The polymer film was ~100 nm thick.

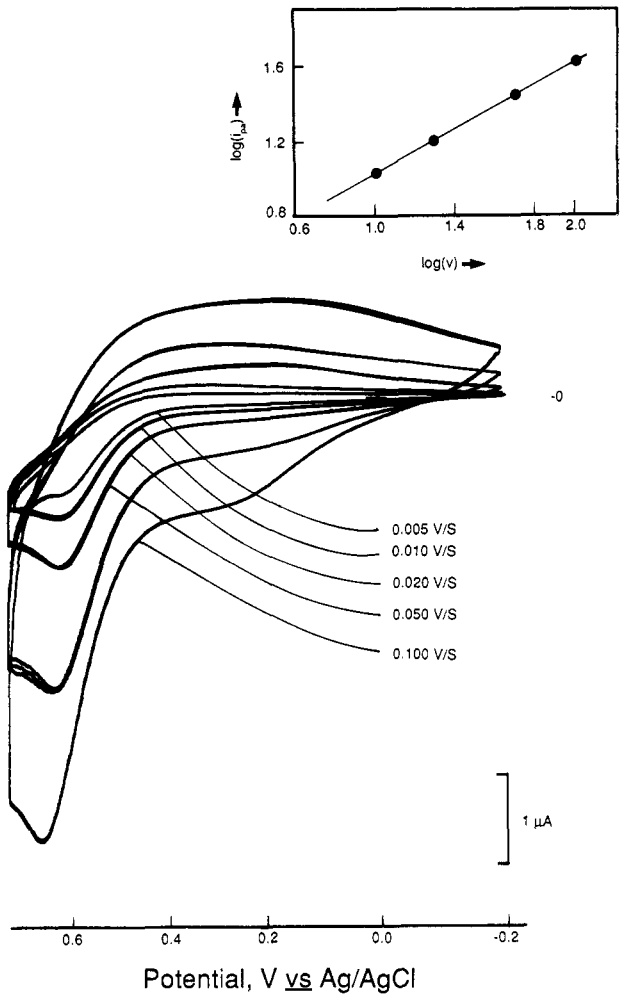

Figure 7. Cyclic voltammograms at varying scan rates for a Pt-supported poly-2 film (thickness: ~80 nm) in MeCN/0.1 M TBAP containing 1 mM ferrocene. The inset shows a log–log plot of the peak current (i_{pa}) for ferrocene oxidation versus the scan rate (v).

redox species, respectively. The latter values pertain strictly to a planar surface and do not take into account surface roughness effects.[51] We attribute the measured departure of the slope from the 0.5 value to such effects. An alternative possibility is permeation of the ferrocene probe into the poly-2 pore structure followed by electron transfer at the substrate/film interphase. There is literature precedent for such effects.[52]

Photophysical Behavior of Poly-1 and Poly-2. The original incentive for this work was the possibility that polymers derived from 1 and 2 could be used to reversibly and electrochemically modulate the luminescent emission of fluorophoric moieties (such as anthracene) attached to them.[31] This strategy would have implications for fluorooptic sensor applications. Preliminary tests, however, reveal strong quenching of the anthracene emission in polymer films derived from 1 and 2. In these experiments, particular care was taken (via for example by Soxhlet extraction) to remove any adsorbed monomer from the polymer films. An added complication is the bond cleavage that ensues when the polymer films are redox-switched in a suitable medium between +0.70 and −0.90 V. For example, a strong emission signal was observed when poly-2 was electrochemically reduced and reoxidized in MeCN/0.1 M TBAP. We suspect that cleavage of the anthracene moiety from the polymer backbone occurs under such conditions.

Thus, the available evidence on poly-1 and poly-2 suggests the microenvironment of the fluorophores to be drastically different from that existing in the thin-layer cell geometry and Au-minigrid-supported polypyrrole membranes, which were employed in our previous study.[31] The coupling (both optical as well as energy transfer) between the fluorophore and the polymer backbone is presumably too strong in the structures of poly-1 and poly-2 to permit effective electrochemical modulation to occur. It is also possible that the *effective* fluorophore concentration in poly-1 and poly-2 is so high that concentration quenching would be rather efficient. In this regard, development of the fluorophore-modified polymers by surface derivatization would appear to be a fruitful avenue in that the probe separation is likely to be higher. Alternative dilution strategies utilizing copolymerization of 1 and 2 with other more photophysically inert structures such as polystyrene are currently under investigation. Modifications in the spacer geometry separating the fluorophoric core and the polymer backbone in 1 and 2 are also being pursued in this laboratory. In conclusion, the coupling of theory and experiment as employed in this study has afforded clear delineation of the factors dictating

(51) Nyikos, L.; Pajkossy, T. *Electrochim. Acta* **1985**, *30*, 1533 and references therein.
(52) Bull, R. A.; Fan, F.-R.; Bard, A. J. *J. Electrochem. Soc.* **1982**, *129*, 1009.

the polymerizability of a given monomer system. In particular, we have shown how electronic rather than steric factors are crucial in this regard for the systems considered here. Further, these new polymers bearing a fluorophoric functionality may represent a useful addition to the array of functionalized conducting polymers previously reported.[1-29]

Acknowledgment. This work was supported in part by the Defense Advanced Research Projects Agency (contract monitored by the Office of Naval Research) and by the Robert A. Welch Foundation (Grant Y-743). It is also a pleasure to thank Drs. E. W. Tsai and V. D. Panchalingam for contributions to the voltammetric and NMR experiments.

Anodic Electrosynthesis of CdTe Thin Films

Dong Ham, Kamal K. Mishra, Alex Weiss,† and Krishnan Rajeshwar*

Department of Chemistry, The University of Texas at Arlington, Arlington, Texas 76019

Received July 10, 1989

Cadmium telluride thin films were anodically electrosynthesized by using Cd anodes in an alkaline solution of sodium telluride. Thermodynamic (Pourbaix) analyses predicted that the oxidation of Te^{2-} to CdTe was more favorable relative to the corresponding $Te^{2-} \rightarrow Te^0$ reaction. Hydrodynamic and cyclic voltammetry permitted detailed characterization of the Cd and Te electrochemistry in alkaline media. Cyclic photovoltammetry, wherein a Cd anode was intermittently illuminated with white light during potential cycling, unequivocally showed the formation of a photoelectrochemically responsive n-type CdTe thin film atop the Cd substrate surface. These films were also formed *at open circuit* via an electroless route. The CdTe thin films thus formed were further characterized by their photoaction spectra in alkaline Te^{2-}/Te_2^{2-} electrolyte and by surface analyses including Auger and X-ray photoelectron spectroscopy, scanning electron microscopy, and scanning Auger microscopy. The virtue of the anodic electrosynthesis route in terms of avoiding contamination of CdTe with Te^0 was clearly seen in these surface analysis data, especially when the corresponding results obtained for the cathodically synthesized thin films in these laboratories and elsewhere were compared.

Introduction

Cadmium telluride is an attractive compound semiconductor candidate for many optoelectronic applications.[1] Thin films of this material have been synthesized by a variety of techniques including vacuum evaporation, sputtering, close-spaced vapor transport, screen printing, spray pyrolysis, and chemical vapor deposition.[2] We[3-6] and others[7-10] have described the advantages of electrochemical syntheses in applications (e.g., solar, switching) wherein thin films with large electro- and photoactive areas are required. In these studies, a cathodic technique involving the codeposition of Cd^{2+} and $HTeO_2^+$ (or molecular Te in the case of nonaqueous media; cf. ref 11) was utilized. In principle, an anodic route ought to be possible involving a Cd anode and oxidizable Te^{2-} species in alkaline media. However, we are not aware of any successful attempts in the case of CdTe, although anodic techniques have been previously utilized for the synthesis of CdS,[12-17] PbS,[18,19] HgS,[20] and Bi_2S_3[12,13,21,22] thin films. We describe in this paper the electrodeposition chemistry and characterizaton of anodically electrosynthesized CdTe thin films. Thermodynamic (Pourbaix) analyses, cyclic and hydrodynamic voltammetry, cyclic photovoltammetry,[23] photoelectrochemical, and surface analyses are described for these thin films.

The second important finding in this work is an anodic *electroless* route to the synthesis of n-CdTe thin films, i.e., formation of n-type CdTe when a Cd anode is held at open circuit in an alkaline Te^{2-} solution. We will show how fairly stoichiometric CdTe may be electrosynthesized in this manner without admixture with Te as a separate phase

Table I. Glossary of Important Electrochemical Reactions in the Anodic Cd–Te System

	reaction	potential, V vs SCE
(1a)	$CdO + 2H^+ + 2e^- = Cd + H_2O$	−1.02
(1b)	$Cd(OH)_2 + 2e^- = Cd + 2OH^-$	−1.06
(2)	$HCdO_2^- + 3H^+ + 2e^- = Cd + 2H_2O$	0.58
(3)	$Te_2^{2-} + 2e^- = 2Te^{2-}$	−1.68
(4)	$Te + 2e^- = Te^{2-}$	−1.38
(5)	$2Te + 2e^- = Te_2^{2-}$	−1.06
(6)	$TeO_3^{2-} + 3H_2O + 4e^- = Te + 6OH^-$	−0.82
(7)	$TeO_4^{2-} + H_2O + 2e^- = TeO_3^{2-} + 2OH^-$	−0.33
(8)	$2TeO_3^{2-} + 12H^+ + 10e^- = Te_2^{2-} + 6H_2O$	0.25
(9)	$TeO_3^{2-} + 3H_2O + 6e^- = Te^{2-} + 6OH^-$	−1.04
(10)	$CdTe + 2e^- = Te^{2-} + Cd$	−1.86

† Department of Physics.

* Author to whom correspondence should be addressed.

(1) Zanio, K. *Semiconductors and Semimetals*; Academic Press: New York, 1978; Vol. 13.
(2) For example: *Proceedings of the IEEE Photovoltaic Specialists' Conference*; IEEE, New York.
(3) Bhattacharya, R. N.; Rajeshwar, K.; Noufi, R. N. *J. Electrochem. Soc.* **1984**, *131*, 939.
(4) Bhattacharya, R. N.; Rajeshwar, K. *J. Electrochem. Soc.* **1984**, *131*, 2032.
(5) Bhattacharya, R. N.; Rajeshwar, K.; Noufi, R. N. *J. Electrochem. Soc.* **1985**, *132*, 732.
(6) Bhattacharya, R. N.; Rajeswar, K. *J. Appl. Phys.* **1985**, *58*, 3590.
(7) Panicker, M. P. R.; Knaster, M.; Kröger, F. A. *J. Electrochem. Soc.* **1978**, *125*, 566.
(8) Fulap, G.; Doty, M.; Meyers, P.; Betz, J.; Liu, C. H. *Appl. Phys. Lett.* **1982**, *40*, 327.
(9) Tukahashi, M.; Uosaki, K.; Kita, H.; Yamaguchi, S. *J. Appl. Phys.* **1986**, *60*, 2046.
(10) Basol, B. M. *Solar Cells* **1988**, *23*, 69.

0897-4756/89/2801-0619$01.50/0